THE JOURNAL OF PHYSICAL CHEMISTRY B LETTERS

2006, *110,* 12839−12842
Published on Web 06/13/2006

Selective Adsorption and Alignment Behaviors of Double- and Multiwalled Carbon Nanotubes on Bare Au and SiO_2 Surfaces

Jiwoon Im, Juwan Kang, Minbaek Lee, Byeongju Kim, and Seunghun Hong*

Physics and Nano-Systems Institute, Seoul National University, Seoul 151-747, Korea

Received: April 6, 2006; In Final Form: May 26, 2006

We present the study of selective adsorption and alignment behaviors of double- and multiwalled carbon nanotubes (dwCNTs and mwCNTs) on self-assembled monolayer (SAM) patterns, bare Au, and SiO_2 surfaces. dwCNTs and mwCNTs exhibited stronger affinity to polar SAMs, bare Au, and SiO_2 surfaces than to nonpolar SAM surfaces. Furthermore, we found the adsorption probability of smaller carbon nanotubes (CNTs) was higher than that of larger CNTs. As proof of concept, we successfully assembled and aligned dwCNTs and mwCNTs on Au and SiO_2 substrates without relying on external forces and demonstrated wafer-scale fabrication of back-gate transistors based on dwCNTs with a high yield.

Advanced devices based on carbon nanotubes (CNTs) and other nanowires (NWs) are drawing the attention of many researchers.[1−7] However, their practical applications have been plagued by a lack of mass-production methods. Previous successful methods for NW assembly include the flow cell method,[8] electric field-induced alignment,[9] directed-growth from catalyst patterns,[10] capillary force-driven assembly,[11,12] aligned growth on miscut crystalline surfaces,[13] etc. However, it is often very difficult to control both the location and orientation of individual CNT patterns over large substrate area using these methods. Recently, a directed-assembly process based on direct interactions between single-walled CNTs (swCNTs) and self-assembled monolayer (SAM) patterns was utilized for large-scale assembly of swCNTs without using external forces.[14−16] However, it was still uncertain whether the same method can be applied to large CNTs such as double- and multiwalled CNTs (dwCNTs and mwCNTs). Herein, we report the study of adsorption and alignment behaviors of dwCNTs and mwCNTs on SAMs, bare Au, and SiO_2 surfaces. dwCNTs and mwCNTs showed strong adhesion to polar SAMs, bare Au, and SiO_2 surfaces, while nonpolar SAMs efficiently prevented CNT adsorption. Furthermore, smaller CNTs were found to have higher adsorption probabilities. As proof of concept, we successfully assembled and aligned dwCNTs and mwCNTs on Au and SiO_2 substrates and demonstrated wafer-scale fabrication of back-gate transistors based on dwCNTs. This result shows that molecular patterns can be utilized to direct assembly of large CNTs without relying on external forces for large-scale device integration.

Figure 1 shows our experimental procedure. First, we patterned nonpolar methyl-terminated SAMs on Au or SiO_2 substrates while leaving some bare surface regions. The bare surface regions could be utilized to adsorb CNTs, or they could be back-filled with polar SAMs. We utilized 1-octadecanethiol (ODT) and octadecyltrichlorosilane (OTS) as a nonpolar SAM on Au and SiO_2, respectively. A 16-mercaptohexadecanoic acid (MHA) SAM terminated with carboxylic acid groups was utilized as a polar SAM on Au. The molecular patterning was performed via dip-pen nanolithography (DPN),[17−25] microcontact printing (MCP),[26] or photolithography,[15] as reported before. In this work, DPN was utilized for initial process development, and we used MCP to generate large-scale ODT patterns on Au. Photolithography was used to create OTS patterns on SiO_2 surface.[15]

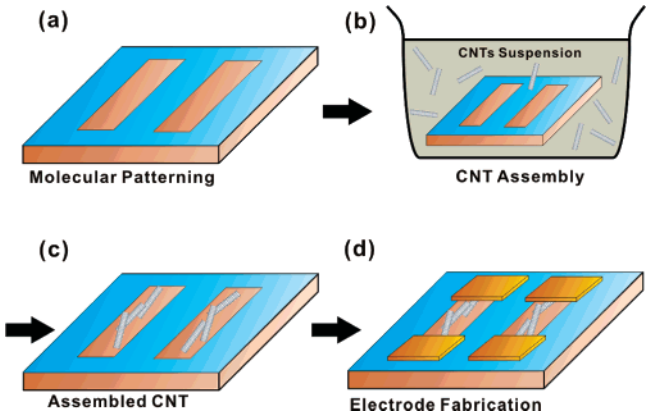

Figure 1. Schematic diagram depicting our assembly procedure of dwCNTs and mwCNTs. (a) Patterning of nonpolar methyl-terminated SAM while leaving some bare surface regions. The bare Au or SiO_2 surface regions could be used for CNT adsorption as it is, or they could be back-filled with polar SAMs (e.g., MHA on Au). (b) Assembly and alignment of CNTs directed by the SAM patterns. (c) Rinsing with *o*-dichlorobenzene leaves CNT patterns. (d) Additional microfabrication process to fabricate electrodes.

When the substrate was placed in the CNT solution (∼0.2 mg/mL in *o*-dichlorobenzene unless specified otherwise) for ∼10 s, CNTs were attracted toward the polar SAM or bare surface regions and aligned along the regions (Figure 1b). It should be noted that the CNTs were aligned only by SAM patterns without any external forces. The substrate was then rinsed with *o*-dichlorobenzene to remove any extra CNTs

* Corresponding author. E-mail: shong@phya.snu.ac.kr

10.1021/jp062146b CCC: $33.50

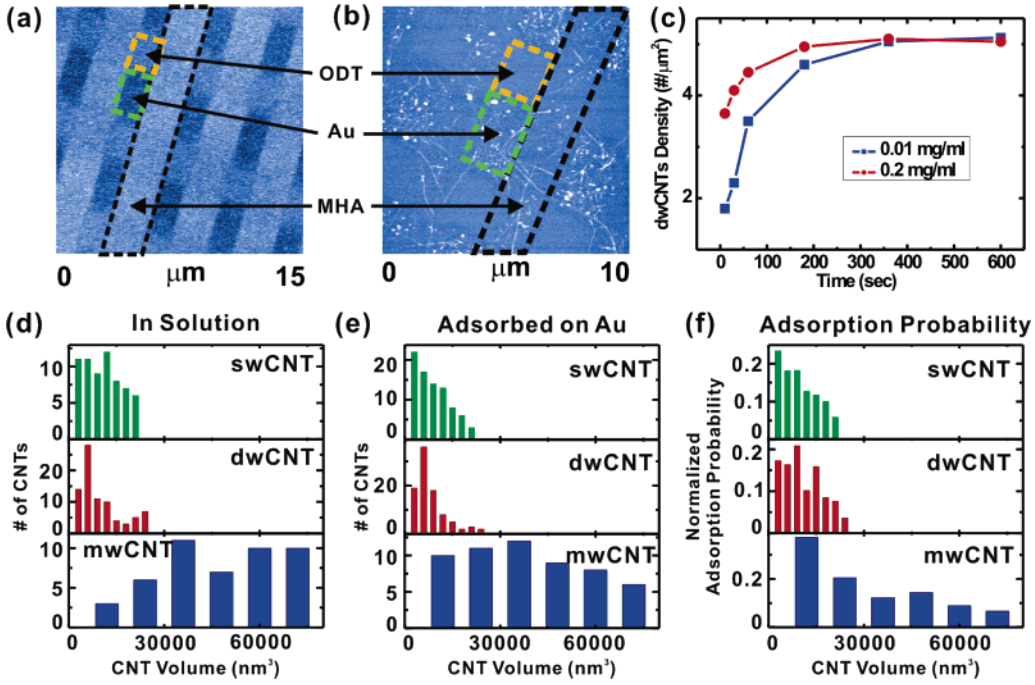

Figure 2. (a) Atomic force microscopy (AFM) topography image of SAM patterns consisting of MHA, ODT, and bare Au regions. The *y*-axis scale is the same as the *x*-axis scale. (b) AFM topography image of dwCNTs assembled onto patterned substrates in Figure 2a. The *y*-axis scale is the same as the *x*-axis scale. (c) Graph showing the number density of dwCNTs adsorbed onto bare Au regions as a function of the time period during which the Au substrate was placed in CNT suspensions (0.01 mg/mL or 0.2 mg/mL in *o*-dichlorobenzene). Each data point represents the average of the number density data measured from five 2 μm $\times$ 2 μm square-shape Au regions. (d) Representative volume distribution of CNTs in our CNT solution. (e) Representative volume distribution of CNTs adsorbed onto bare Au surfaces. (f) Normalized adsorption probabilities of CNTs on bare Au surface as a function of the CNT volume. Smaller CNTs appear to have higher adsorption probabilities.

(Figure 1c). The swCNTs and dwCNTs were purchased from Carbon Nanotechnology, Inc. mwCNTs were purchased from Nanolab, Inc. Since the adsorbed CNTs formed stable structures, we could continue additional processes for device fabrication (Figure 1d). In this report, we utilized photolithography followed by lift-off steps to fabricate electrodes on the CNT patterns.[15] Electrodes were deposited via thermal evaporation (20 nm Au after 10 nm Ti unless specified otherwise).

Figure 2a and b show a typical adsorption behavior. Here, we first prepared SAM patterns comprised of MHA, ODT, and bare Au regions (Figure 2a) by cross-stamping ODT over MHA SAM patterns (Supporting Information). When the substrate was placed in the dwCNT solution, dwCNTs were adsorbed onto both MHA and Au regions, while ODT SAM prevented any nonspecific adsorption (Figure 2b). In previous reports, swCNTs exhibited a strong affinity to amine-terminated SAM patterns.[10] This phenomenon was explained by the electrostatic interactions between positively charged amine groups and negative charges on swCNTs which often occur during common CNT purification processes.[10] In our case, we dispersed our CNTs in *o*-dichlorobenzene, which is a nonpolar organic solvent and does not have a hydrogen bonding domain. Thus, ionic compounds or functional groups cannot be solvated or dissociated in our CNT solution. In this case, the CNTs and SAM surfaces should remain mostly neutral. However, as reported before, under ambient conditions, water molecules are adsorbed onto hydrophilic surfaces and form thin water layers, which allows some surface ions or functional groups to solvate and generates residual surface charges.[27,28] Since ions do not dissolve in *o*-dichlorobenzene, we can expect a small amount of residual charges (generated by air exposure of our substrates) on the polar surfaces remain, even in the CNT solution. We found that CNTs in *o*-dichlorobenzene had a strong affinity to virtually general polar surfaces including relatively neutral bare Au surfaces, while nonpolar SAM blocked CNT adhesion. It implies that the surface charges on the polar SAM patterns were not a dominant factor in our adsorption process. The attractive forces between CNTs and polar surfaces were more likely van der Waals-type attractions. On the other hand, we found CNTs in *o*-dichlorobenzene exhibited a relatively stronger affinity to Au surfaces than MHA SAM surfaces, even though the polarization of MHA SAM was stronger than that of bare Au (Figure 2b). Presumably, the repulsive forces, though very weak, between residual negative charges of MHA SAM and CNTs reduced the affinity of CNTs onto MHA SAM.

Figure 2c shows the time-dependent adsorption behavior of dwCNTs on bare Au surfaces. Here, bare Au surface was placed in the dwCNT solution for different time periods, and the number density of adsorbed dwCNTs was measured using AFM topography images. Significantly, the result shows that the dwCNT adsorption slowed as the number density of adsorbed dwCNTs increased, implying the adsorbed CNTs block additional CNT adsorption. This sounds somewhat contradicting to previous reports where hydrophobic CNT surfaces attracted other CNT surfaces in aqueous solution. The strong affinity of hydrophobic CNT surfaces to other hydrophobic surfaces in water was explained by "hydrophobic attraction" between two polar surfaces. The hydrophobic attraction is originated from the hydrogen bonding between water molecules, and it is usually much stronger than van der Waals forces.[29] However, hydrophobic attraction exists only in aqueous solution. Since we are using nonpolar solvent such as *o*-dichlorobenzene, the hydrophobic attraction does not exist in our system, and the attractive forces between hydrophobic surfaces should be minimal. This also explains why hydrophobic CNTs were not adsorbed onto hydrophobic SAM patterns. The CNT solution concentration affected the adsorption speed. However, the number densities

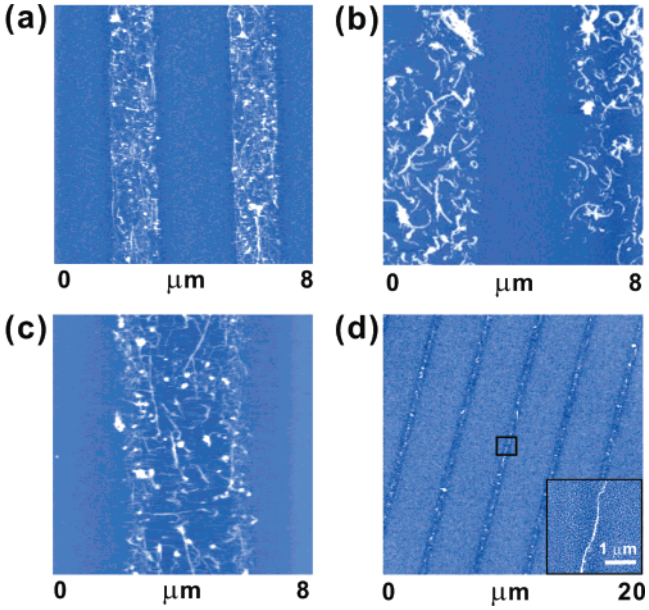

Figure 3. (a) AFM topography image of dwCNT patterns on Au surface. The dwCNTs are adsorbed onto bare Au regions, while ODT SAM blocks CNT adsorption. (b) AFM topography image of mwCNT patterns on Au surface. ODT SAM was utilized for passivation. (c) AFM topography image of dwCNTs adsorbed on SiO_2 substrate. OTS SAM was utilized for passivation. (d) AFM topography image of nanoscale lines of dwCNTs adsorbed onto bare Au surface. Note that dwCNTs were precisely aligned along the bare Au regions (dark areas), while ODT SAM (bright regions) prevented any CNT adsorption. The *y*-axis scales of all AFM images are the same as their *x*-axis scales.

of CNTs adsorbed from two different concentration CNT suspensions eventually reached the similar saturation values.

We also studied size-dependent adsorption probabilities of CNTs on bare Au surfaces (Figure 2d−f). Here, we first deposited ~10 μL CNT solution (0.05 mg/mL in *o*-dichlorobenzene) on Au surfaces using a micropipet and dried to prepare CNT thin films. Then, 125 μm^2 area of the CNT film was imaged via AFM and the number of the CNTs in a specific volume range was counted. The result gave us the representative volume distribution of CNTs in our CNT solution (Figure 2d). On the other hand, we also prepared CNT films by dipping Au surfaces in the same CNT solution for 10 s. By repeating the same AFM analysis, we obtained the representative volume distribution of CNTs adsorbed onto bare Au surfaces (Figure 2e). To calculate the normalized adsorption probability, the adsorption probability of CNTs was first calculated by dividing the number of adsorbed CNTs (Figure 2e) by that of CNTs in the solution (Figure 2d), and then it was normalized so that their total sum over entire volume ranges becomes one (Figure 2f). The result shows that smaller CNTs have a higher adsorption probability. Presumably, larger CNTs in solution moved slower than smaller ones, and they had less probability to hit the substrate.

Using this strategy, we successfully demonstrated precision adsorption and alignment of dwCNTs and mwCNTs over large area (~1 cm × 1 cm) on Au and SiO_2 substrates (Figure 3). Significantly, Figure 3b shows that our assembly method can be applied to mwCNTs as large as 30 nm in diameter. We can also apply the same strategy to SiO_2 substrates (Figure 3c). In this case, polar SiO_2 surfaces with hydroxyl groups exhibited an affinity strong enough to attract large CNTs. Please note that CNTs did not cross the pattern boundaries, and they were confined in the bare surface regions. We could achieve high-precision alignment of CNTs using nanoscale line-shape patterns

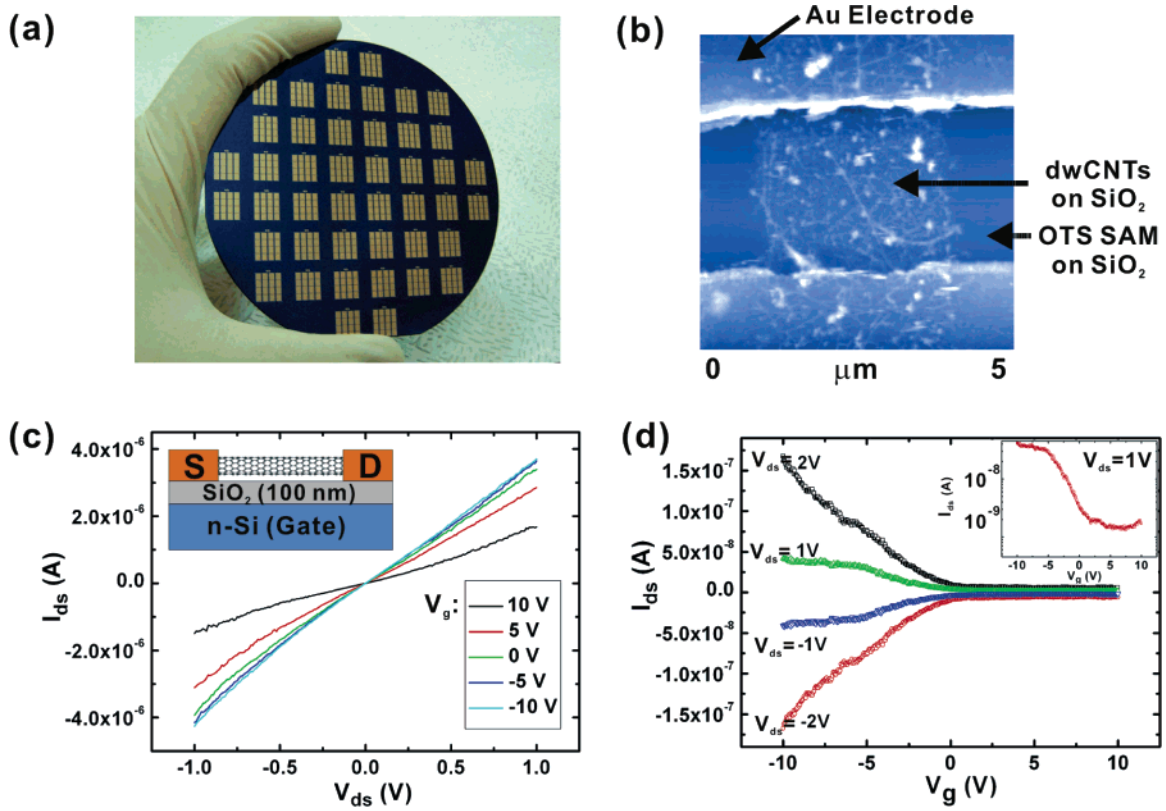

Figure 4. (a) Photograph image showing a wafer containing 528 back-gate transistors based on dwCNT patterns. (b) AFM topography image of dwCNT patterns connecting source and drain electrodes in the back-gate transistor. The *y*-axis scale is the same as *x*-axis scale. (c) Source−drain voltage sweeps of a dwCNT transistor under various gate biases showing a typical p-type behavior. (d) Gate voltage sweeps of a dwCNT transistor under various source−drain voltages V_{ds}. Inset shows the log scale plot of gate voltage sweep with $V_{ds} = 1$ V.

(Figure 3d). Here, dwCNTs were directly adsorbed onto bare Au surfaces while ODT SAM blocked CNT adsorption. We also achieved high precision alignment of dwCNTs using MHA patterns generated via DPN (Supporting Information).

Since CNTs adsorbed onto bare surfaces formed stable structures, we could continue additional microfabrication steps for large-scale fabrication of integrated devices (Figure 4). Here, an OTS SAM was first patterned on 100 nm-thick SiO_2 layer while leaving some bare SiO_2 surface. Then, dwCNTs were selectively adsorbed onto the bare SiO_2 surface, and electrodes were fabricated on top of the adsorbed dwCNT patterns via conventional lift-off methods. Here, the underlying n-type Si substrate could be used as a back-gate to measure the gating effect. Using this process, we successfully performed wafer-scale fabrication of back-gate transistors (Figure 4a and b). Although we demonstrated individual-CNT-level control in Figure 3d, the resolution of the wafer-scale process is still limited by that of current photolithography methods. However, recent reports show the possibility of high-yield nanofabrication methods,[18,30] which gives us high prospects for fabricating single tube field-effect transistor (FET) with a high yield using this strategy.

Figure 4c and d show the electrical characterization of a dwCNT transistor using the underlying n-type Si substrate as a back-gate. The data show typical behaviors of p-type transistors based on dwCNTs under ambient conditions. Since our transistors were comprised of dwCNT networks containing both metallic and semiconducting dwCNTs, they did not turn off completely. The gating effect varied depending on junctions due to the different composition of metallic and semiconducting dwCNTs. We had only one disconnected junction out of tested two hundred dwCNT junctions, showing the reliability of our process. The resistance of connected dwCNT junctions varied depending on the adsorbed CNT densities and materials used for electrodes. For example, the resistance of 100 dwCNT junctions with Pd electrodes varied between 4 kΩ $\sim$ 40 kΩ, while those with Ti/Au electrodes had resistance values between 20 kΩ $\sim$ 85 kΩ.

In summary, we report the study of the selective adsorption and precision alignment behaviors of relatively large dwCNTs and mwCNTs on SAM, bare Au, and bare SiO_2 surfaces. dwCNTs and mwCNTs exhibited strong adsorption onto bare Au, SiO_2, and polar SAMs, while nonpolar SAMs efficiently blocked their adsorption. Smaller CNTs were found to have higher adsorption probability to polar surfaces than larger CNTs. As proof of concept, we successfully assembled dwCNTs and mwCNTs over large substrate area and demonstrated wafer-scale fabrication of back-gate transistors.

Acknowledgment. This project has been supported by KOSEF through NRL and Samsung Electronics. S.H. also acknowledges the partial support from the TND program.

Supporting Information Available: A method to generate SAM patterns consisting of MHA, ODT, and bare Au regions and dwCNTs assembled on DPN-generated MHA patterns. These materials are available free of charge via the Internet at http://pubs.acs.org.

References and Notes

(1) Iijima, S. *Nature* **1991**, *354*, 56.

(2) Javey, A.; Guo, J.; Wang, Q.; Lundstrom, M.; Dai, H. *Nature* **2004**, *424*, 654.

(3) Duan, X.; Niu, C.; Sahi, V.; Chen, J.; Parce, J. W.; Empedocles, S.; Goldman, J. L. *Nature* **2003** *425*, 274.

(4) Frank, S.; Poncharal, P.; Wang, Z. L.; de Heer, W. A. *Science* **1998**, *280*, 1744.

(5) Cui, Y.; Wei, Q.; Park, H.; Lieber, C. M. *Science* **2001** *293*, 1289.

(6) Hata, K.; Futaba, D. N.; Mizuno, K.; Namai, T.; Yumura, M.; Iijima, S. *Science* **2004**, *306*, 1362.

(7) de Pablo, P. J.; Graugnard, E.; Walsh, B.; Andres, R. P.; Datta, S.; Reifenberger, R. *Appl. Phys. Lett.* **1999**, *74*, 323.

(8) Huang, Y.; Duan, X.; Wei, Q.; Lieber, C. M. *Science* **2001**, *291*, 630.

(9) Zhang, Y.; Chang, A.; Cao, J.; Wang, Q.; Kim, W.; Li, Y.; Morris, N.; Yenilmez, E.; Kong, J.; Dai, H. *Appl. Phys. Lett.* **2001**, *79*, 3155.

(10) Liu, J.; Casavant, M. J.; Cox, M.; Walters, D. A.; Boul, P.; Lu, W.; Rimberg, A. J.; Smith, K. A.; Colbert, D. T.; Smalley, R. E. *Chem. Phys. Lett.* **1999**, *303*, 125.

(11) Wang, Y.; Maspoch, D.; Zou, S.; Schatz, G. C.; Smalley, R.; Mirkin, C. A. *Proc. Natl. Acad. Sci. U.S.A.* **2006**, *103*, 2026.

(12) Oh, S. J.; Cheng, Y.; Zhang, J.; Shimoda, H.; Zhou, O. *Appl. Phys. Lett.* **2003**, *82*, 2521.

(13) Kocabas, C.; Hur, S. H.; Gaur, A.; Meitl, M. A.; Shim, M.; Rogers, J. A. *Small* **2005**, *1*, 1110.

(14) Rao, S. G.; Huang, L.; Setyawan, W.; Hong, S. *Nature* **2003**, *425*, 36.

(15) Myung, S.; Lee, M.; Kim, G. T.; Ha, J. S.; Hong, S. *Adv. Mater.* **2005**, *17*, 2361.

(16) Hannon, J. B.; Afzali, A.; Klinke, Ch.; Avouris, Ph. *Langmuir* **2005**, *21*, 8569.

(17) Piner, R. D.; Zhu, J.; Xu, F.; Hong, S.; Mirkin, C. A. *Science* **1999**, *283*, 661.

(18) Hong, S.; Mirkin, C. A. *Science* **2000**, *288*, 1808.

(19) Maynor, B. W.; Li, Y.; Liu, J. *Langmuir* **2001**, *17*, 2575.

(20) Manandhar, P.; Jang, J.; Schatz, G. C.; Ratner, M. A.; Hong, S. *Phys. Rev. Lett.* **2003**, *90*, 115505.

(21) Cho, N.; Ryu, S.; Kim, B.; Schatz, G. C.; Hong, S. *J. Chem. Phys.* **2006**, *124*, 24714.

(22) Nyamjav, D.; Ivanisevic, A. *Adv. Mater.* **2003**, *15*, 1805.

(23) Jaschke, M.; Butt, H. J. *Langmuir* **1995**, *11*, 1061.

(24) Sheehan, P. E.; Whitman, L. J. *Phys. Rev. Lett.* **2002**, *88*, 156104.

(25) Coffey, D. C.; Ginger, D. S. *J. Am. Chem. Soc.* **2005**, *127*, 4564.

(26) Xia, Y.; Whitesides, G. M. *J. Am. Chem. Soc.* **1995**, *117*, 3274.

(27) Lee, N. K.; Hong, S. *J. Chem. Phys.* **2006**, *124*, 114711.

(28) Pashley, R. M. *J. Colloid Interface Sci.* **1981**, *83*, 531.

(29) Israelachvili, J. *Intermolecular and Surface Forces*; Academic Press: New York, 1992.

(30) Jansson, P. A. C.; Hansson, B. A. M.; Hemberg, O.; Otendal, M.; Holmberg, A.; de Groot, J.; Hertz, H. M. *Appl. Phys. Lett.* **2004**, *84*, 2256.